Chapter 12
Intracranial Aneurysms: Modeling Inception and Enlargement

Paul N. Watton, Haoyu Chen, Alisa Selimovic, Harry Thompson, and Yiannis Ventikos

Abstract Intracranial aneurysms (IAs) are abnormal dilatations of the cerebral vasculature. Computational modeling may shed light on the aetiology of the disease and lead to improved criteria to assist diagnostic decisions. We briefly review the literature and present novel models on two topical areas of research activity: modeling IA inception and modeling IA evolution. We present a novel computational methodology to remove an IA and reconstruct the geometry of the (unknown) healthy artery. This approach is applied to 22 clinical cases (the largest study of its kind to date) and we analyze whether spatial distributions of hemodynamic stimuli correlate with locations aneurysms are known, a priori, to form. In this study, locations of aneurysm formation are strongly correlated with regions of high wall shear stress (WSS) (19/22 positive correlations); however low correlations are observed with indices which characterize the oscillatory nature of the direction of the wall shear stress vector, e.g., oscillatory shear index (OSI) (7/22). We subsequently outline a fluid-solid-growth framework for modeling aneurysm evolution and illustrate its application to 4 clinical cases depicting IAs. We conclude with a discussion for the direction of future research in this field.

12.1 Introduction

Intracranial aneurysms (IAs) appear as sac-like outpouchings of the arterial wall inflated by the pressure of the blood. Prevalence rates in populations without comor-

P.N. Watton (✉) · H. Chen · A. Selimovic · H. Thompson · Y. Ventikos
Institute of Biomedical Engineering, Department of Engineering Science, University of Oxford, Oxford, UK
e-mail: Paul.Watton@eng.ox.ac.uk

H. Chen
e-mail: Haoyu.Chen@eng.ox.ac.uk

A. Selimovic
e-mail: Alisa.Selimovic@eng.ox.ac.uk

Y. Ventikos
e-mail: Yiannis.Ventikos@eng.ox.ac.uk

bidity are estimated to be 3.2 % (Vlak et al., 2011). Most remain asymptomatic; however, there is a small but inherent risk of rupture: 0.1 to 1 % of detected aneurysms rupture every year (Juvela, 2004). Subarachnoid haemorrhage (SAH) due to IA rupture is associated with a 50 % chance of fatality (Greving et al., 2009) and of those that survive, nearly half have long term physical and mental sequelae (Huang et al., 2011). Preemptive treatment may prevent aneurysm SAH and thus reduce the associated (large) financial burden, e.g., the total annual economic cost of aneurysm SAH is £510 M in the UK (Rivero-Arias et al., 2010). However, management of unruptured IAs by interventional procedures, i.e. minimally invasive endovascular approaches or surgical-clipping, is highly controversial and not without risk (Komotar et al., 2008). Given the very low risk of IA rupture, there is both a clinical and an economic need to identify those IAs which are actually in need of intervention.

Investigating the complex interplay of physical forces and their biological sequelae will aid further understanding of the formation and rupture of IAs and their management, and may lead to a cure (Krings et al., 2011). However, IAs may have heterogeneous hemodynamic, morphologic, and vascular characteristics associated with different mechanistic pathways (Sugiyama et al., 2011) and thus this is an extremely challenging complex problem. Computational models may yield insight into the aetiology of the disease and offer the potential to aid clinical decisions. Consequently, research in this area has grown extensively; for recent review articles see, e.g., Humphrey (2009); Sforza et al. (2011). In this article, we briefly review computational models which investigate IA inception and IA evolution and present our most recent models and findings on these topical areas of research.

12.2 IA Inception

IAs preferentially develop at specific locations in the Circle of Willis. Hence it appears that the hemodynamic environment plays a role in the pathophysiological processes that give rise to their formation. This has motivated the development of methodologies to reconstruct the original *healthy* geometry of the vasculature from a *diseased* geometry depicting an IA: computational fluid dynamic (CFD) analyzes proceed to investigate if particular patterns of hemodynamic stimuli (on the healthy vasculature) correlate with the location at which an IA is observed to develop, e.g., see the recent studies by Mantha et al. (2006); Baek et al. (2009); Ford et al. (2009); Shimogonya et al. (2009); Singh et al. (2010). Whilst all these studies have considered a limited number of clinical cases, i.e. between 1 and 5, interesting (although somewhat inconsistent) observations have been made (see Table 12.1). It has been concluded that locations susceptible to aneurysm formation are associated with: oscillatory wall shear stress (WSS) indicated by a novel index referred to as the aneurysm formation index (AFI) (Mantha et al., 2006); large temporal fluctuations of the direction of the spatial WSS gradient vector (WSSG) indicated by a novel index referred to as the gradient oscillatory number (GON) (Shimogonya

Table 12.1 Summary of IA inception studies. The spatial distributions of various hemodynamic indices have been compared with known locations of aneurysm formation. It can be seen that strong correlations are always observed in such studies. However, inconsistencies in conclusions are present and the study sizes are always small

Study	CFD index	Positive correlation
Mantha et al. (2006)	Low WSS, AFI	3/3
Shimogonya et al. (2009)	GON	1/1
Ford et al. (2009)	GON	4/5
Baek et al. (2009)	High WSS, High Pressure	2/2
Singh et al. (2010)	High WSS, High OSI	2/2

et al., 2009); elevated WSS and pressure (Baek et al., 2009); elevated WSS and oscillatory shear index (OSI) (Singh et al., 2010); the interested reader is referred to the relevant articles for specifics of how to calculate these hemodynamic indices.

Given the disparates in findings on CFD inception studies to date, there is clearly the need for a more comprehensive study: we consider a selection of 22 sidewall IAs, propose a novel method to reconstruct the hypothetical geometry of the artery without IA and analyze spatial distributions of hemodynamic stimuli on the healthy vasculature in the specific locations that the IAs are known, a priori, to develop.

12.2.1 Methodology

We have developed a novel approach to reconstruct the hypothetical geometry of the healthy artery prior to IA formation. Here we briefly outline the methodology (see Fig. 12.1 for graphical illustration). Clinical imaging data depicting an IA is segmented with the software suite @neufuse (developed for the European project @neurIST, www.aneurist.org 'Integrated Biomedical Informatics for the Management of Cerebral Aneurysms', see Villa-Uriol et al., 2011). A skeleton of the vasculature is created and the segment containing the IA is removed (see Fig. 12.1(b)). Given the position vectors of the center points of the upstream and downstream boundaries (neighboring the aneurysm section), $\mathbf{c}_0$ and $\mathbf{c}_1$, respectively, and unit normal vectors to the boundaries $\hat{\mathbf{n}}_0$ and $\hat{\mathbf{n}}_1$ (see Fig. 12.1(c)), a cubic curve $\mathbf{c}(t) = (a_{1j}t^j, a_{2j}t^j, a_{3j}t^j): i = 1, 2, 3; j = 0, 1, 2, 3; t \in [0, 1]$ is constructed such that

$$\mathbf{c}(t = 0) = \mathbf{c}_0, \qquad \mathbf{c}(t = 1) = \mathbf{c}_1, \qquad \mathbf{c}'(t = 0) = \kappa\hat{\mathbf{n}}_0, \qquad \mathbf{c}'(t = 1) = \kappa\hat{\mathbf{n}}_1, \tag{12.1}$$

where $\prime$ denotes differentiation with respect to t and $\kappa = |\mathbf{c}_1 - \mathbf{c}_0|$. The 12 unknown coefficients $a_{ij} \in \mathbb{R}$ are uniquely determined by the 12 boundary conditions given by Eq. (12.1). A Frenet-Frame is then defined along the curve $\mathbf{c}$, i.e.

$$\mathbf{T}(t) = \frac{\mathbf{c}'(t)}{|\mathbf{c}'(t)|}, \qquad \mathbf{N}(t) = \frac{\mathbf{T}'(t)}{|\mathbf{T}'(t)|}, \qquad \mathbf{B}(t) = \mathbf{T}(t) \times \mathbf{N}(t). \tag{12.2}$$
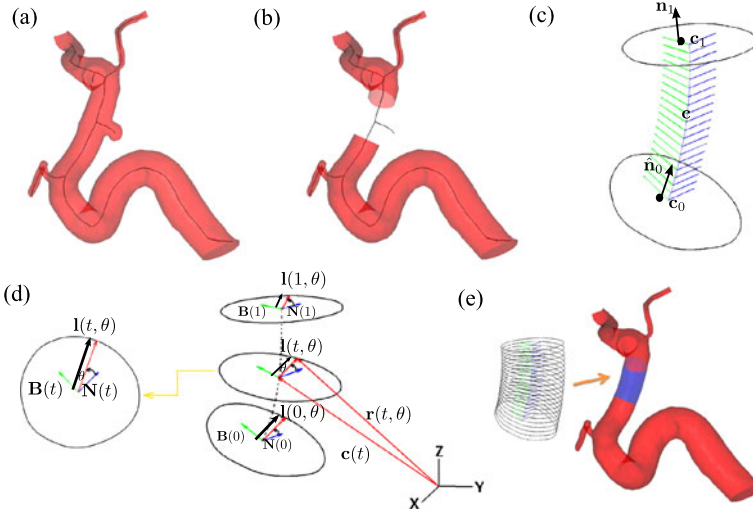
Fig. 12.1 Methodology to remove sidewall IA and reconstruct original healthy vessel: (**a**) segmented clinical image of vasculature depicting IA; (**b**) removal of section containing IA; (**c**) a Frenet-Frame is constructed along a curve $\mathbf{c}(s)$ between the upstream and downstream boundaries of the segment containing the IA that was removed; (**d**) methodology to smoothly morph the inlet boundary into the outlet boundary along $\mathbf{c}$; (**e**) reconstructed healthy vessel

The hypothetical healthy geometry is reconstructed by using the Frenet-Frame to propagate a closed curve in the **N**–**B** plane along $\mathbf{c}$ such that the upstream boundary smoothly morphs into the downstream boundary. This approach takes into account the natural tortuosity of the artery. The vector equation of the reconstructed healthy section of arterial surface $\mathbf{r}(t,\theta)$, $\theta \in [0, 2\pi)$ can be expressed as

$$\mathbf{r}(t,\theta) = \mathbf{c}(t) + \mathbf{l}(t,\theta), \tag{12.3}$$

where $\mathbf{l}(t,\theta)$ represents the position vectors of points on the boundary in the $\mathbf{N}(t)$–$\mathbf{B}(t)$ plane along $\mathbf{c}$. $\mathbf{l}(0,\theta)$ and $\mathbf{l}(1,\theta)$ are determined from the known position vectors of the upstream and downstream boundaries and we choose $\mathbf{l}(t,\theta)$ to be a linear combination of these:

$$\mathbf{l}(t,\theta) = \big|(1-t)\mathbf{l}(0,\theta) + t\mathbf{l}(1,\theta)\big|(\mathbf{N}\cos\theta + \mathbf{B}\sin\theta). \tag{12.4}$$

This novel reconstruction method is applied to 22 clinical cases depicting sidewall IAs. Figure 12.2 illustrates the application of the approach to 20 (segmented) clinical cases; the geometry of the IA is depicted in light blue whilst the geometry of the reconstructed segment of healthy artery is in depicted in dark blue.

12.2.1.1 Computational Fluid Dynamics

The methodological approach to solve the hemodynamics proceeds as follows. The geometry of the artery without IA is imported into ANSYS ICEM (ANSYS Inc.,
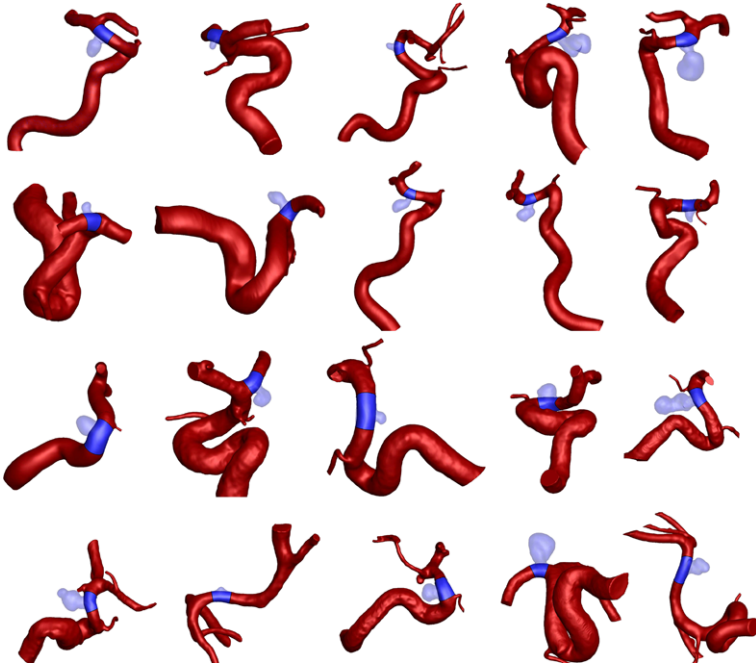
Fig. 12.2 An illustration of 20 cases with/without IAs. The reconstructed section is depicted in *dark blue* whilst the IA is depicted in *light blue*

Canonsburg, PA) and an unstructured tetrahedral mesh with prism layers lining the boundary is generated for the fluid domain. Blood is modeled as an incompressible Newtonian fluid with constant density $\rho = 1069\,\text{kg}\,\text{m}^{-3}$ and viscosity $\eta = 0.0035\,\text{Pa}\,\text{s}$. At the arterial wall, no slip, no-flux conditions are applied. Pulsatile flow and pressure boundary conditions for the inlets and outlets of the fluid domain are taken from a 1D model of the arterial tree (Reymond et al., 2009) which has been integrated into the software suite @neufuse. It solves the 1D form of the Navier-Stokes equation in a distributed model of the human systemic arteries, accounting for the ventricular-vascular interaction and wall viscoelasticity; it was recently validated through a comparison with in vivo flow measurements (Reymond et al., 2011). The incompressible Navier-Stokes equations which govern the flow are solved with ANSYS CFX (ANSYS Inc., Canonsburg, PA) using a finite volume formulation.

12.2.2 Results

CFD simulations are performed on 22 clinical cases with IAs removed. Spatial distributions of several hemodynamic indices are analyzed and compared with respect
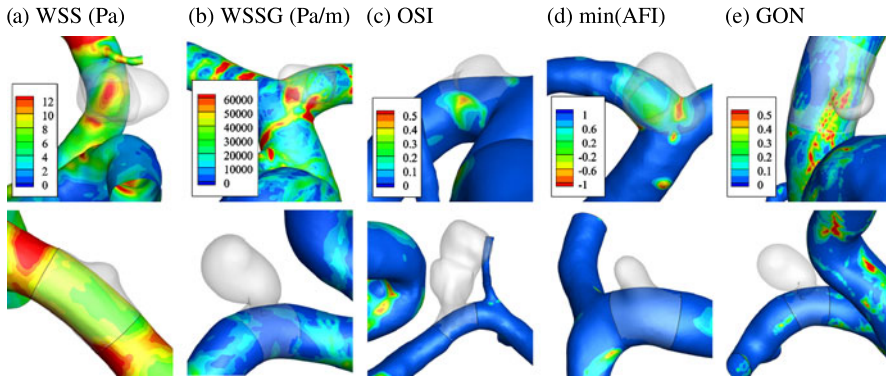
Fig. 12.3 Examples of spatial distributions of (**a**) WSS, (**b**) WSSG, (**c**) OSI, (**d**) min(AFI) and (**e**) GON (*left* to *right*, respectively) for reconstructed healthy vessels without IAs. The *upper row* illustrates cases where a positive correlation between an index and the location an IA evolves occurs whilst the *lower row* illustrates examples where no correlation is observed

to the known locations of aneurysm formation (LAF). Figure 12.3 illustrates examples of positive (upper row) and negative (lower row) correlations of the hemodynamic indices WSS, WSSG, OSI, minimum(AFI) and GON with the LAF. We observed that 19/22 IAs developed in regions that had locally elevated magnitudes of WSS and GON. However, fewer positive correlations were observed for other indices, i.e. 7/22 for elevated values of OSI, 7/22 for low values of min(AFI) and 8/22 for elevated values of WSSG.

Our study highlights that care should be taken when interpreting the conclusions and findings of smaller CFD studies in the literature. For example, we observed that low values of AFI were associated with 7/22 clinical cases whereas Mantha et al. (2006) observed correlations in all cases (3/3). Singh et al. (2010) observed a significant correlation with OSI (2/2) however we observed no such correlation. Consistent with Baek et al. (2009) we observed a positive correlation with regions subject to high WSS. Whilst we observed many positive correlations (19/22) with elevated GON, as observed and remarked by Ford et al. (2009), this index is elevated in many regions of the artery and thus the significance of this correlation is unclear and may merit further investigation.

12.3 IA Enlargement

To further our understanding of the aetiology of IA we must further our understanding of the physiological mechanisms that regulate the maintenance of arterial tissue in physiological and pathophysiological conditions. The structure of the artery is continually maintained by vascular cells. The morphology and functionality of vascular cells is intimately linked to their mechanical environment. Hemodynamic forces give rise to: cyclic stretching of the extra-cellular matrix (ECM); frictional

forces acting on the endothelial layer of the arterial wall; a normal hydrostatic pressure and interstitial fluid forces due to movement of fluid through the ECM. Mechanosensors convert the mechanical stimuli into chemical signals which lead to activation of genes that regulate cell functionality. The physiological mechanisms that give rise to the development of an aneurysm involve the complex interplay between the local mechanical forces acting on the arterial wall and the biological processes occurring at the cellular level. Consequently, models of aneurysm evolution must take into consideration: (i) the biomechanics of the arterial wall; (ii) the biology of the arterial wall and (iii) the complex interplay between (i) and (ii), i.e. the mechanobiology of the arterial wall. Humphrey and Taylor (2008) recently emphasized the need for a new class of fluid-solid-growth models to study aneurysm evolution and proposed the terminology FSG models. These combine fluid and solid mechanics analyzes of the vascular wall with descriptions of the kinetics of biological growth and remodeling (G&R).

12.3.1 Methodology

In this section, we describe our FSG computational framework for modeling IA evolution. It utilizes and extends the novel abdominal aortic aneurysm (AAA) evolution model developed by Watton et al. (2004) and Watton and Hill (2009) which was later adapted to model IA evolution (Watton et al., 2009b; Watton and Ventikos, 2009) and extended to consider transmural variations in G&R (Schmid et al., 2010, 2011). The aneurysm evolution model incorporates microstructural G&R variables into a realistic structural model of the arterial wall (Holzapfel et al., 2000). These describe the *normalized mass-density* and *natural reference configurations* of the load bearing constituents, and enable the G&R of the tissue to be simulated as an aneurysm evolves. More specifically, the natural reference configurations that collagen fibers are recruited to load bearing remodels to simulates the mechanical consequences of: (i) fiber deposition and degradation in altered configurations as the aneurysm enlarges; (ii) fibroblasts configuring the collagen to achieve a maximum strain during the cardiac cycle, denoted the attachment strain. The normalized mass-density evolves to simulate growth/atrophy of the constituents (elastin and collagen). The aneurysm evolution model has been integrated into a novel FSG framework (Watton et al., 2009a) so that G&R can be explicitly linked to hemodynamic stimuli. More recently, the G&R framework has been extended to link both *growth* and *remodeling* to cyclic deformation of vascular cells (see Watton et al., 2012).

Figure 12.4 depicts the FSG methodology. The computational modeling cycle begins with a structural analysis to solve the systolic and diastolic equilibrium deformation fields (of the artery/aneurysm) for given pressure and boundary conditions. The structural analysis quantifies the stress, stretch, and the cyclic deformation, of the constituents and vascular cells (each of which may have different natural reference configurations). The geometry of the aneurysm is subsequently exported to be prepared for hemodynamic analysis: first the geometry is integrated into a physiological geometrical domain; the domain is automatically meshed; physiological
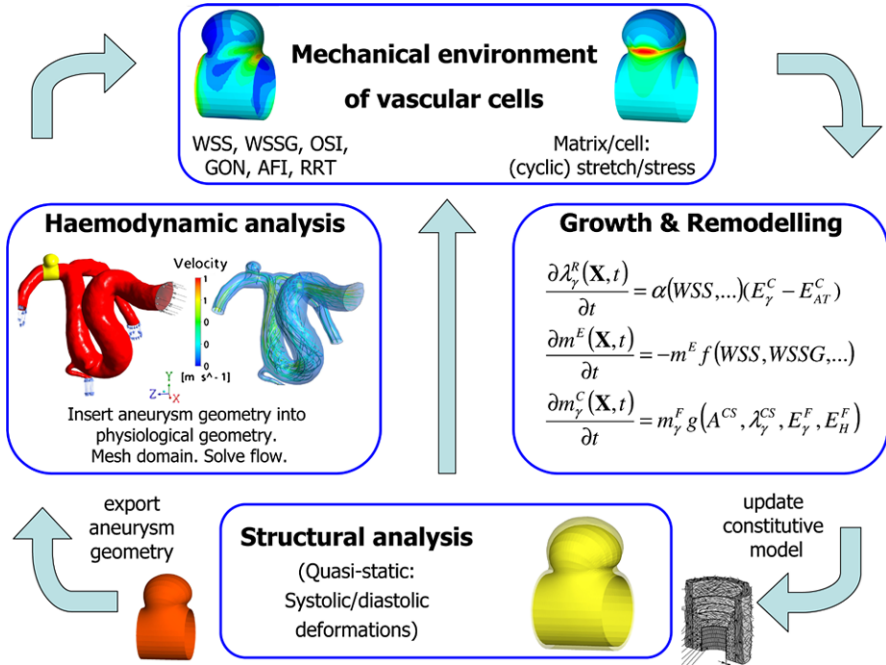
Fig. 12.4 Fluid-solid-growth computational framework for modeling aneurysm evolution

flow rate and pressure boundary conditions are applied; the flow is solved assuming rigid boundaries for the hemodynamic domain. The hemodynamic quantities of interest, e.g., WSS, WSSG are then exported and interpolated onto the nodes of the structural mesh: each node of the structural mesh contains information regarding the mechanical stimuli obtained from the hemodynamic and structural analyzes. G&R algorithms simulate cells responding to the mechanical stimuli and adapting the tissue: the constitutive model of the aneurysmal tissue is updated. The structural analysis is re-executed to calculate the new equilibrium deformation fields. The updated geometry is exported for hemodynamic analysis. The cycle continues and as the tissue adapts an aneurysm evolves.

Development of an IA is associated with apoptosis of vascular smooth muscle (VSM) cells (Kondo et al., 1998), disrupted internal elastic laminae, the breakage and elimination of elastin fibers (Frösen et al., 2004), a thinned medial layer and G&R of the collagen fabric (Juvela, 2004). The site of origin is strongly related to hemodynamic WSS (Kondo et al., 1997). It is postulated that high WSS is related to the initiation of IA formation (Ahn et al., 2007); note that this hypothesis is consistent with our observations in Sect. 12.2. However, whilst high WSS appears to be associated with the inception of an IA, low WSS is thought to give rise to its continued enlargement (Shojima et al., 2004).

To simulate IA inception, we prescribe a localized loss of elastin in a small circular patch of the arterial domain (the elastin is modeled with a neo-Hookean con-

stitutive model Watton et al., 2009c). The collagen fabric adapts to restore home-ostasis and a small perturbation to the geometry alters the spatial distribution of hemodynamic stimuli that act on the lumenal layer of the artery. This enables sub-sequent degradation of elastin to be linked to deviations of hemodynamic stimuli from homeostatic levels via evolution equations. As the elastin degrades and the collagen fabric adapts (via G&R) an IA evolves. Watton et al. (2009a) adopted this approach to investigate the evolution of IAs assuming degradation of elastin was linked to high WSS or high WSSG. Given that a region of elevated WSS occurs downstream of the distal neck of the model IA and elevated spatial WSSGs occur in the proximal/distal neck regions, this approach led to IAs that enlarged axially along the arterial domain, i.e. it did not yield IA with characteristic 'berry' topolo-gies. Consequently, Watton et al. (2011a) linked elastin degradation to low WSS and restricted the degradation of elastin to a localized region of the arterial domain: this yielded IAs of a characteristic saccular shape that enlarged and stabilized in size. Although interesting insights were obtained in both studies, an inherent limitation was that the IAs evolved on a cylindrical section of artery and consequently the spa-tial distribution of hemodynamic stimuli is non-physiological. This motivated the application of the FSG modeling framework to patient-specific vascular geometries. For a detailed description of the model methodology, we refer the interested reader to Watton et al. (2011b, 2012). Here we briefly illustrate the application of the FSG modeling framework to 4 clinical cases.

12.3.2 Examples of FSG Models of IA Evolution

Figure 12.5 (upper row) illustrates 4 clinical cases depicting IAs. The IA is removed (as in Fig. 12.1(b)) and replaced with a short cylindrical section on which IA evo-lution is simulated. The cylindrical section is smoothly reconnected to the upstream and downstream sections of the parent artery (middle row; see Selimovic et al., 2010, for methodology). In all four cases, IA inception is prescribed, i.e. an initial degradation of elastin is prescribed in a localized region of the domain, the collagen fabric adapts to restore homeostasis and a small localized outpouching of the artery develops. This perturbs the hemodynamic environment: subsequent degradation of elastin is linked to low levels of WSS. It can be seen that the modeling framework gives rise to IAs with different morphologies, i.e. IAs with: asymmetries in geome-tries (a_3, d_3); well-defined necks (b_3); no neck (c_3). For an in depth analysis of simulation results for case (a_3), e.g., evolution of elastin strains, collagen strains, concentrations of constituents and evolving diastolic/systolic geometries, the inter-ested reader is referred to Watton et al. (2011b). Interestingly, for this particular case, which depicts an IA at (perhaps) a relatively early stage of formation (crudely inferred from its small size), the qualitative asymmetries of the simulated IA (see (a_3)) are in agreement with the patient aneurysm (a_1) and thus (tentatively) support the modeling hypotheses for elastin degradation (low WSS drives degradation) and collagen adaption.
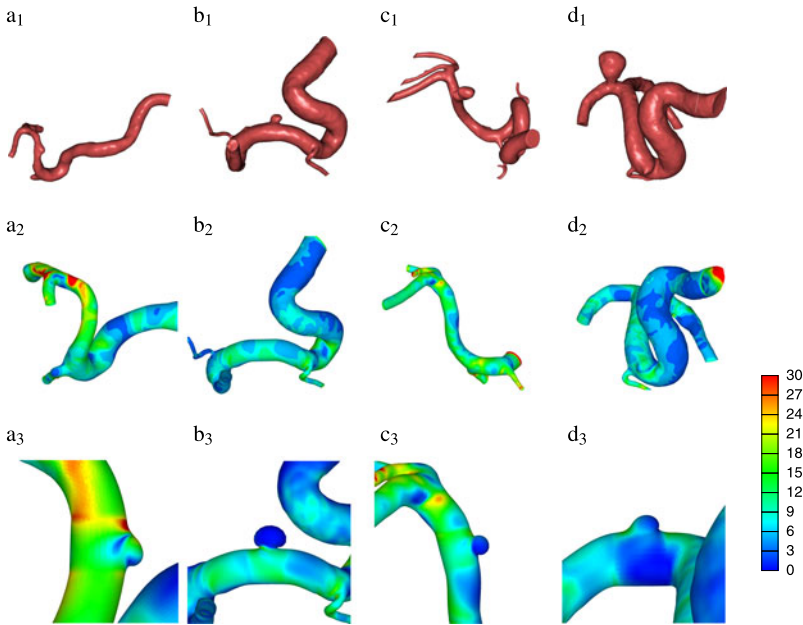
Fig. 12.5 Segmented clinical imaging data depicting IAs (a_1–d_1). IAs are removed the geometry of the healthy artery reconstructed (a_2–d_2). Computational models of IAs on patient specific geometries with degradation of elastin linked to low WSS (a_2–d_2). The color-map depicts WSS (Pa)

12.4 Discussion

In this chapter, we first (briefly) reviewed the application of CFD models to investigate IA inception and presented a novel methodology for reconstructing the geometry of the healthy artery prior to IA formation. We investigated the correlation between IA inception and the spatial distribution of several hemodynamic indices (WSS, WSSG, OSI, AFI and GON) for 22 clinical cases depicting sidewall IAs. To our knowledge this is the largest (and most complete) CFD inception study, of its kind, to date. Consistent with previous observations, we observed that locations of aneurysm formation (LAF) occur in regions of the artery subject to high WSS. However, correlation of LAF with indices that characterize the oscillatory nature of the flow, i.e. OSI and min(AFI), do not seem as strong as (sometimes) previously observed. Hence, we suggest care should be taken: (i) when interpreting conclusions of studies which have been deduced from a small number of clinical cases; (ii) articulating the significance of conclusions of CFD studies which involve relatively few cases. Moreover, we point out that whilst CFD has a role to play in guiding our understanding of vascular disease, it needs to be coupled with improved modeling (and understanding) of the mechanobiology of the arterial wall to gain real insight into the aetiology of vascular disease. This motivates the need for multi-scale models which integrate the biology and the (solid and fluid) biomechanics of the arterial

wall, i.e. FSG models, such as the one we presented. Such models provide the foundations to model not only aneurysm evolution but other vascular diseases.

It is envisaged that models of IA and AAA evolution may ultimately lead to predictive models that have diagnostic application on a patient specific basis. Given that this will yield very substantial healthcare and economic benefits, there is significant growth of research in this area. However, whilst models of aneurysm evolution have gained increasing sophistication over the past decade, many further improvements are still required. For instance, there is a need to incorporate explicit representations of vascular cells (endothelial cells, fibroblast cells and smooth muscle cells), their interactions and the signaling networks (Schmid et al., 2011) that link the stimuli acting on them to their functionality in physiological, supra-physiological and pathological conditions. There is also a need for implementation of more sophisticated constitutive models to represent, e.g., the collagen fiber recruitment distribution (Hill et al., 2012) and dispersion and the active and passive response of vascular smooth muscle cells (Murtada et al., 2010). Lastly, improved understanding and modeling of how this complex micro-structure adapts in pathological conditions is needed: the modeling framework needs to be validated and/or calibrated against physiological data; animal models undoubtedly have a role to play in this respect (Zeng et al., 2011). Such enhancements will offer the potential for patient-specific predictive models of vascular disease evolution and intervention. They will benefit patients immensely because the decision on whether to/how to intervene will be founded upon a robust concentration of knowledge with respect to patient-specific vascular physiology, biology and biomechanics. Of course, the challenging and multi-disciplinary nature of such research implies collaborations are essential.

References

Ahn S, Shin D, Tateshima S, Tanishita K, Vinuela F, Sinha S (2007) Fluid-induced WSS in anthropomorphic brain aneurysm models: MR phase-contrast study at 3T. J Musculoskel Neuron Interact 25:1120–1130

Baek H, Jayaraman MV, Karniadakis GE (2009) Wall shear stress and pressure distribution on aneurysms and infundiblae in the posterior communicating artery bifurcation. Ann Biomed Eng 37:2469–2487

Ford MD, Hoi Y, Piccinelli M, Antiga L, Steinman DA (2009) An objective approach to digital removal of saccular aneurysms: technique and applications. Br J Radiol 82:S55–S61

Frösen J, Piippo A, Paetau A, Kangasniemi M, Niemelä M, Hernesniemi J, Jääskeleläinen J (2004) Remodelling of saccular cerebral artery aneurysm wall is associated with rupture: histological analysis of 24 unruptured and 42 ruptured cases. Stroke 35:2287–2293

Greving JP, Rinkel GJE, Buskens E, Algra A (2009) Cost-effectiveness of preventive treatment of intracranial aneurysms: new data and uncertainties. Stroke 73:258–265

Hill MR, Duan X, Gibson GA, Watkins S, Robertson AM (2012) A theoretical and non-destructive experimental approach for direct inclusion of measured collagen orientation and recruitment into mechanical models of the artery wall. J Biomech 45:762–771

Holzapfel GA, Gasser TC, Ogden RW (2000) A new constitutive framework for arterial wall mechanics and a comparative study of material models. J Elast 61:1–48

Huang MC, Baaj AA, Downes K, Youssef AS, Sauvageau E, van Loveren HR, Agazzi S (2011) Paradoxical trends in the management of unruptured cerebral aneurysms in the united states. Stroke 42:1730–1735

Humphrey JD (2009) Coupling haemodynamics with vascular wall mechanics and mechanobiology to understand intracranial aneurysms. Int J Comput Fluid Dyn 23:569–581

Humphrey JD, Taylor CA (2008) Intracranial and abdominal aortic aneurysms: similarities, differences, and need for a new class of computational models. Annu Rev Biomed Eng 10:221–246

Juvela S (2004) Treatment options of unruptured intracranial aneurysms. Stroke 35:372–374

Komotar RJ, Mocco J, Solomon RA (2008) Guidelines for the surgical treatment of unruptured intracranial aneurysms: the first annual J. Lawrence pool memorial research symposium-controversies in the management of cerebral aneurysms. Neurosurgery 62:183–194

Kondo S, Hashimoto N, Kikuchi H, Hazama F, Nagata I, Kataoka H (1997) Cerebral aneurysms arising at nonbranching sites. An experimental study. Stroke 28:398–403

Kondo S, Hashimoto N, Kikuchi H, Hazama F, Nagata I, Kataoka H, Rosenblum WI (1998) Apoptosis of medial smooth muscle cells in the development of saccular cerebral aneurysms in rats. Stroke 29:181–189

Krings T, Mandell DM, Kiehl TR, Geibprasert S, Tymianski M, Alvarez H, terBrugge KG, Hans FJ (2011) Intracranial aneurysms: from vessel wall pathology to therapeutic approach. Neurosurgery 7:547–559

Mantha A, Karmonik C, Benndorf G, Strother C, Metcalfe R (2006) Hemodynamics in a cerebral artery before and after the formation of an aneurysm. Am J Neuroradiol 27:1113–1118

Murtada S, Kroon M, Holzapfel GA (2010) A calcium-driven mechanochemical model for prediction of force generation in smooth muscle. Biomech Model Mechanobiol 9:749–762

Reymond P, Merenda F, Perren F, Rüfenacht D, Stergiopulos N (2009) Validation of a one-dimensional model of the systemic arterial tree. Am J Physiol, Heart Circ Physiol 297:H208–H222

Reymond P, Bohraus Y, Perren F, Lazeyras F, Stergiopulos N (2011) Validation of a patient-specific one-dimensional model of the systemic arterial tree. Am J Physiol, Heart Circ Physiol 301:H1173–H1182

Rivero-Arias O, Gray A, Wolstenholme J (2010) Burden of disease and costs of aneurysmal subarachnoid haemorrhage (aSAH) in the united kingdom. Cost Eff Resour Allocation 8:6

Schmid H, Grytsan A, Postan E, Watton PN, Itskov M (2011) Influence of differing material properties in media and adventitia on arterial adaption: application to aneurysm formation and rupture. Comput Methods Biomech Biomed Eng. doi:10.1080/10255842.2011.603309

Schmid H, Watton PN, Maurer MM, Wimmer J, Winkler P, Wang YK, Roehrle O, Itskov M (2010) Impact of transmural heterogeneities on arterial adaptation: application to aneurysm formation. Biomech Model Mechanobiol 9:295–315

Selimovic A, Villa-Uriol M-C, Holzapfel GA, Ventikos Y, Watton PN (2010) A computational framework to explore the role of the pulsatile haemodynamic environment on the development of cerebral aneurysms for patient-specific arterial geometries. In: Lim CT, Goh JCH (eds) 6th world congress of biomechanics (WCB 2010), IFMBE proceedings, vol 31. Springer, Berlin, pp 759–762

Sforza DM, Putman CM, Cebral JR (2011) Computational fluid dynamics in brain aneurysms. Int J Numer Methods Biomed Eng 28:801–808

Shimogonya Y, Ishikawa T, Imai Y, Matsuki N, Yamaguchi T (2009) Can temporal fluctuation in spatial wall shear stress gradient initiate a cerebral aneurysm? A proposed novel hemodynamic index, the gradient oscillatory number (GON). J Biomech 42:550–554

Shojima M, Oshima M, Takagi K, Torii R, Hayakawa M, Katada K, Morita A, Kirino T (2004) Magnitude and role of WSS on cerebral aneurysm: computational fluid dynamic study of 20 middle cerebral artery aneurysms. Stroke 35:2500–2505

Singh PK, Marzo A, Howard B, Rufenacht DA, Bijlenga P, Frangi AF, Lawford PV, Coley SC, Hose DR, Patel UJ (2010) Effects of smoking and hypertension on wall shear stress and oscilla-

tory shear index at the site of intracranial aneurysm formation. Clin Neurol Neurosurg 112:306–313

Sugiyama SI, Meng H, Funamoto K, Inoue T, Fujimura M, Nakayama T, Omodaka S, Shimizu H, Takahashi A, Tominaga T (2011) Hemodynamic analysis of growing intracranial aneurysms arising from a posterior inferior cerebellar artery. World Neurosurg. doi:10.1016/j.wneu.2011.09.023

Villa-Uriol MC, Berti G, Hose DR, Marzo A, Chiarini A, Penrose J, Pozo J, Schmidt JG, Singh P, Lycett R, Larrabide I, Frangi AF (2011) @neurIST complex information processing toolchain for the integrated management of cerebral aneurysms. Inter Focus 1:308–319

Vlak MH, Algra A, Brandenburg R, Rinkel GJ (2011) Prevalence of unruptured intracranial aneurysms, with emphasis on sex, age, comorbidity, country, and time period: a systematic review and meta-analysis. Lancet Neurol 10:626–636

Watton PN, Hill NA (2009) Evolving mechanical properties of a model of abdominal aortic aneurysm. Biomech Model Mechanobiol 8:25–42

Watton PN, Ventikos Y (2009) Modelling evolution of saccular cerebral aneurysms. J Strain Anal 44:375–389

Watton PN, Hill NA, Heil M (2004) A mathematical model for the growth of the abdominal aortic aneurysm. Biomech Model Mechanobiol 3:98–113

Watton PN, Raberger NB, Holzapfel GA, Ventikos Y (2009a) Coupling the hemodynamic environment to the evolution of cerebral aneurysms: computational framework and numerical examples. J Biomech Eng 131:101003

Watton PN, Ventikos Y, Holzapfel GA (2009b) Modelling the growth and stabilisation of cerebral aneurysms. Math Med Biol 26:133–164

Watton PN, Ventikos Y, Holzapfel GA (2009c) Modelling the mechanical response of elastin for arterial tissue. J Biomech 42:1320–1325

Watton PN, Selimovic A, Raberger NB, Huang P, Holzapfel GA, Ventikos Y (2011a) Modelling evolution and the evolving mechanical environment of saccular cerebral aneurysms. Biomech Model Mechanobiol 10:109–132

Watton PN, Ventikos Y, Holzapfel GA (2011b) Modelling cerebral aneurysm evolution. In: McGloughlin T (ed) Biomechanics and mechanobiology of aneurysms. Springer, Heidelberg, pp 373–399

Watton PN, Huang H, Ventikos Y (2012) Multi-scale modelling of vascular disease: abdominal aortic aneurysm evolution. Springer, Heidelberg

Zeng Z, Kallmes DF, Durka MJ, Ding Y, Lewis DA, Kadirvel R, Robertson AM (2011) Hemodynamics and anatomy of elastase-induced rabbit aneurysm models-similarity to human cerebral aneurysms? Am J Neuroradiol 32:595–601